Journal of Solid State Chemistry 181 (2008) 1456–1461

Contents lists available at ScienceDirect

Journal of Solid State Chemistry

journal homepage: www.elsevier.com/locate/jssc

Fluorescence and phosphorescence properties of the low temperature forms of the $MAl_2Si_2O_8:Eu^{2+}$ (M = Ca, Sr, Ba) compounds

Frédéric Clabau [a], Alain Garcia [b], Pierre Bonville [c], Danielle Gonbeau [d], Thierry Le Mercier [e], Philippe Deniard [a], Stéphane Jobic [a,*]

[a] Institut des Matériaux Jean Rouxel, Université de Nantes, CNRS, 2 rue de la Houssinière, BP 32229, 44340 Nantes, France
[b] Institut de Chimie de la Matière Condensée de Bordeaux, UPR 9048, 87 avenue du Dr. Albert Schweitzer, 33608 Pessac Cedex, France
[c] Commissariat à l'Energie Atomique, Centre d'Etudes de Saclay, Service de Physique de l'Etat Condensé, 91191 Gif-sur-Yvette, France
[d] LCTPCM, UMR 5624, Helioparc Pau Pyrénées, 2 avenue Pierre Angot, 64053 Pau Cedex 9, France
[e] RHODIA, Centre de Recherches d'Aubervilliers, 52 rue de la Haie-Coq, 93308 Aubervilliers cedex, France

ARTICLE INFO

Article history:
Received 7 November 2007
Received in revised form
13 March 2008
Accepted 13 March 2008
Available online 25 March 2008

Keywords:
$MAl_2Si_2O_8$ (M = Ca, SrBa)
Fluorescence
Phosphorescence
Defect conglomeration

ABSTRACT

The fluorescence and phosphorescence properties of Europium-doped $MAl_2Si_2O_8$ (M = Ca, Sr, Ba) are reinvestigated and discussed on the basis of the propensity of an activator to agglomerate with an oxygen vacancy. Due to a stronger attraction of the anion vacancy towards Eu^{2+} cations going from $BaAl_2Si_2O_8$ to $SrAl_2Si_2O_8$ and $CaAl_2Si_2O_8$ host lattices, the interpretation of the fluorescence spectra turns out to be less trivial in the Ca and Sr host lattices than in the Ba one and requests the account for Eu^{2+} cations lying at alkaline-earth sites with or without vacancy in their neighborhood. Phosphorescence in these compounds is highlighted.

1. Introduction

Since the discovery of the outstanding, long-lasting afterglow (hereafter also called phosphorescence and persistent luminescence) of $SrAl_2O_4:Eu^{2+},Dy^{3+},B^{3+}$ in 1995 by Murayama et al. [1], Eu^{2+}-doped aluminates, silicates or aluminosilicates received a strong incentive in order to stabilize new persistent luminescent materials. Concurrently, numerous investigations were dedicated to the understanding and the rationalization of the mechanisms at the origin of phosphorescence in these families of materials [2–9]. This ended at the now, well-accepted consensus that the persistent luminescence in Eu^{2+}-containing phosphors is based on the photo-ionization of Eu^{2+} into Eu^{3+} under UV–visible illumination with trapping of the photo-generated electrons at defects. For sure, some controversies still exist concerning the chemical nature of these defects. Namely, Clabau et al. [5,7] as Ohta et al. previously [10], proposed to assign these trap levels to oxygen vacancies (or more generally speaking, to oxygen vacancy-based defects) located in the vicinity of the Eu^{2+} activator, the position in energy of the associated levels being strongly influenced by the nature of the codopant due to a defect conglomeration phenomenon. In contrast, Dorenbos [6] preferred to assign the electron traps to rare-earth Ln^{3+} cations, which might be reduced into their Ln^{2+} state with a $4f^{n+1}$ configuration lying just below the conduction band. As debated by Clabau et al. [8] this model suffers from the fact that it cannot explain the intrinsic phosphorescence of un-codoped $SrAl_2O_4:Eu^{2+}$ and that chemical species as Dy^{3+}, Nd^{3+}, Ho^{3+} which favor phosphorescence duration when introduced as codopant are very unstable in oxides in their 2+ oxidation state [11]. This point of view seems to be shared by Aitasalo et al. [9] who sided with Clabau et al. [5,7,8] on the specific point of the conglomeration of oxygen vacancy and codopant Ln^{3+} cations, the defect assembly being favored in their model via the proximity of an alkaline-earth vacancy.

Nowadays, if a large panel of emission colors of the phosphors with phosphorescence lasting longer than 1 h is reported in the literature (e.g. $CaAl_2O_4:Eu^{2+},Nd^{3+},B^{3+}$ [3] and $Sr_4Al_{14}O_{25}:Eu^{2+},Dy^{3+},B^{3+}$ [12] (blue), $SrAl_2O_4:Eu^{2+},Dy^{3+},B^{3+}$ [1] (green), $CdSiO_3:Mn^{2+}$ [13] (orange), $Ca_2Al_2SiO_7:Ce^{3+},Mn^{2+}$ [14] (yellow), $Y_2O_2S:Eu^{3+},Ti^{4+},Mg^{2+}$ [15] (red)), no white, perceived phosphorescence is mentioned. In this context, we have embarked on the (re)investigation of the luminescence properties of the Eu-doped $MAl_2Si_2O_8$ (M = Ca, Sr, Ba) series.

Both $BaAl_2Si_2O_8$ and $SrAl_2Si_2O_8$ materials exist under four crystallographic forms, two of them occurring as natural minerals with a monoclinic symmetry [16]. The most widespread variety,

* Corresponding author. Fax: +33 2 40 37 39 95.
E-mail address: stephane.jobic@cnrs-imn.fr (S. Jobic).

0022-4596/$ - see front matter © 2008 Elsevier Inc. All rights reserved.
doi:10.1016/j.jssc.2008.03.011

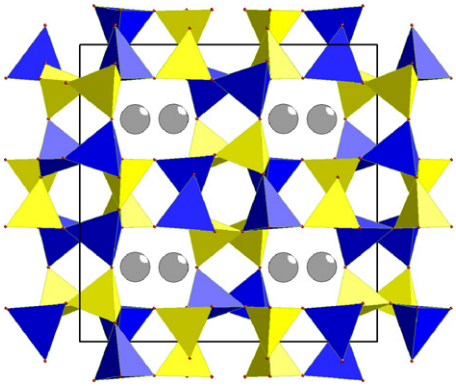

Fig. 1. Schematic views of the $BaAl_2Si_2O_8$ low-temperature form along the *c*-direction. The structures of $CaAl_2Si_2O_8$ and $SrAl_2Si_2O_8$ derive from the celsian-$BaAl_2Si_2O_8$ by a slight distortion ([SiO_4] and [AlO_4] tetrahedra in yellow and blue, respectively; Ba in gray).

called *celsian* (SG: *I*2/*c*), is thermodynamically stable up to 1590 and 1650 °C. The other monoclinic form, labeled *paracelsian* and *slawsonite* (SG: *P*21/*a*) for the Ba and Sr derivatives, has never been stabilized via synthesis routes. The *β-hexacelsian* forms (SG: $P6_3/mcm$ and *P*6/*mmm*) can be obtained at ambient temperature by quenching in air from temperature higher than 1590 and 1650 °C, respectively. This metastable variety may then transform into the *α-hexacelsian* form (SG: *Immm*) below 300 °C under conditions not yet well defined. For its part, $CaAl_2Si_2O_8$ feldspar exists under three crystallographic allotropic forms [17]. The triclinic one, called *anorthite* (SG: *P*-1), is the stable phase while the two others, i.e. the orthorhombic and the hexagonal ones, are metastable.

In the following, we will concentrate our attention on the luminescence properties of the three $MAl_2Si_2O_8$ (M = Ca, Sr, Ba) phases stable at low temperature, i.e. the *celsian* and *anorthite* forms. All of them consist of a 3D network of AlO_4 and SiO_4 tetrahedra bound by vertices, with alkaline-earth cations housed in channels along the three directions (Fig. 1). The aluminum avoidance principle is respected, i.e. each aluminum cation is surrounded by four silicon and vice versa [18]. Ba^{2+} and Sr^{2+} cations occupied a single nine-fold coordinated site, whereas Ca^{2+} cations lie at four two-fold crystallographically independent sites exhibiting either a six-fold or a seven-fold coordination.

Our work is organized as follows. In Section 2, we describe the experimental procedures followed to synthesize powdered $MAl_2Si_2O_8$:Eu^{2+} (M = Ca, Sr and Ba) materials, as well as the physical techniques used to characterize the samples. The fluorescence and phosphorescence properties of the materials are discussed in Sections 3 and 4, respectively. The essential findings of our work are summarized in Section 5.

2. Experimental

$BaCO_3$ (Strem, 5N), $SrCO_3$ (Alfa Aesar, 4N), $CaCO_3$ (Alfa Aesar, 4N), Al_2O_3 (Chempur, 4N), SiO_2 (Chempur, 4N) and Eu_2O_3 (Rhodia Electronics & Catalysis, 4N) were employed as raw materials. Precursors were weighted in stoichiometric amounts, rare-earth cations being expected to substitute for the alkaline-earth cations in the host lattice for steric reasons as usually.

Celsian $BaAl_2Si_2O_8$:Eu^{2+} and $SrAl_2Si_2O_8$:Eu^{2+}, and anorthite $CaAl_2Si_2O_8$:Eu^{2+} were obtained after heating of the starting materials in alumina crucibles in a reducing Ar+5%H_2 atmosphere at 1350 °C for 50, 20 and 50 h, respectively. A preliminary ball milling step of the precursors (2 h at 700 rev/min with a Fritsch Pulverissette 7) was requested to achieve pure celcian $BaAl_2Si_2O_8$ to speed up the sluggish phase transformation of the hexacelsian phase into the celsian form carriage return. The powder X-ray diffraction (XRD) patterns were collected with a Siemens D5000 diffractometer without monochromator (CuK-L_3, $\lambda = 1.540598$ and CuL-L_2, $\lambda = 1.544390$ Å), in a Bragg–Brentano reflection geometry with a linear detector in the 10–100° 2θ range. The purity of all the prepared, powdered materials was systematically checked by XRD. All the diffraction peaks were assigned to the $MAl_2Si_2O_8$:Eu phases (M = Ca, Sr, Ba) as exemplified in Fig. 2 for M = Ca. No characteristic peaks of the dopants were observed after a full pattern matching analysis, which evidence that a solid-state solution is formed in all the samples to be investigated. Chemical compositions were verified by energy dispersive X-ray spectroscopy (EDXS) on a JEOL JSM-5800LV scanning electron microscope coupled with a germanium PGT Prism detector.

Luminescence measurements were carried out at room temperature with a Fluorolog 3 Jobin Yvon spectrofluorimeter equipped with a 450 W Xe lamp as a light source and with a R928P Hamamatsu photomultiplier for photon counting mode or a CCD multichannel detector for instant emission spectra.

Room temperature UV–vis diffuse reflectance spectra of undoped materials were collected on a finely ground sample with a Cary 5G spectrometer (Varian) equipped with a 60 mm diameter integrating sphere and computer control using the "Scan" software. Diffuse reflectance was measured from 250 to 830 nm using Halon powder (from Varian) as reference (100% reflectance).

The ^{151}Eu Mössbauer absorption spectra were recorded using a $^{151}SmF_3$ γ-ray source with activity of 14 GBq, in transmission geometry. The sample mass was about 200 mg, and spectra were recorded at 77 K in order to increase the Lamb–Mössbauer factor, and hence the signal/noise ratio.

The X-ray photoelectron spectra (XPS) were recorded on a Surface Science Instrument spectrometer (model 301) using a focused (diameter of the irradiated area = 600 μm) monochromatized Al $K\alpha$ radiation (1486.6 eV). The residual pressure inside the analysis chamber was ca. 5×10^{-8} Pa. The spectrometer was calibrated by using the photoemission lines of Au (Au $4f_{7/2}$ = 83.9 eV with respect to the Fermi level) and Cu (Cu $2p_{3/2}$ = 932.5 eV). For the Au $4f_{7/2}$ line the full-width at half-maximum was 0.86 eV under the recording conditions. The peaks were recorded with constant pass energy of 50 eV. Charging effects were minimized with a low-energy electron flood gun in conjunction with a transmitting fine mesh proximity screen. The binding energy scale was calibrated from the carbon contamination using the C 1*s* peak at 284.6 eV.

3. Fluorescence of $MAl_2Si_2O_8$:Eu^{2+} (M = Ca, Sr, Ba)

The emission spectra of $MAl_2Si_2O_8$:Eu^{2+} (M = Ca, Sr, Ba) are displayed in Fig. 3. They all consist of a broad and intense band corresponding to the allowed $4f^6 5d^1 \rightarrow 4f^7(^8S_{7/2})$ transition of Eu^{2+}, with a maximum located at 430, 404 and 440 nm, respectively. These values roughly agree with those reported in the literature [19–22]. It is worth noticing that the emission bands in the three $MAl_2Si_2O_8$:Eu materials spread out on a large domain of the visible range, which explains why these phosphors present a bluish white luminescence with naked eyes. The calculated CIE chromatic coordinates for $M_{0.98}Eu_{0.02}Al_2Si_2O_8$ compounds are (0.17,0.12), (0.16,0.09) and (0.16,0.11) for M = Ca, Sr and Ba, respectively (λ_{exc} = 310 nm). It can also be noted that the lack of emission lines characteristic of Eu^{3+} cations does not mean at all that traces of these species do not exist in the samples since the $4f$–$4f$ emissions are forbidden as electric–dipole transitions and are several order of magnitude less intense than the spin and parity allowed Eu^{2+} $5d \rightarrow 4f$ transition. Formally, as evidenced by

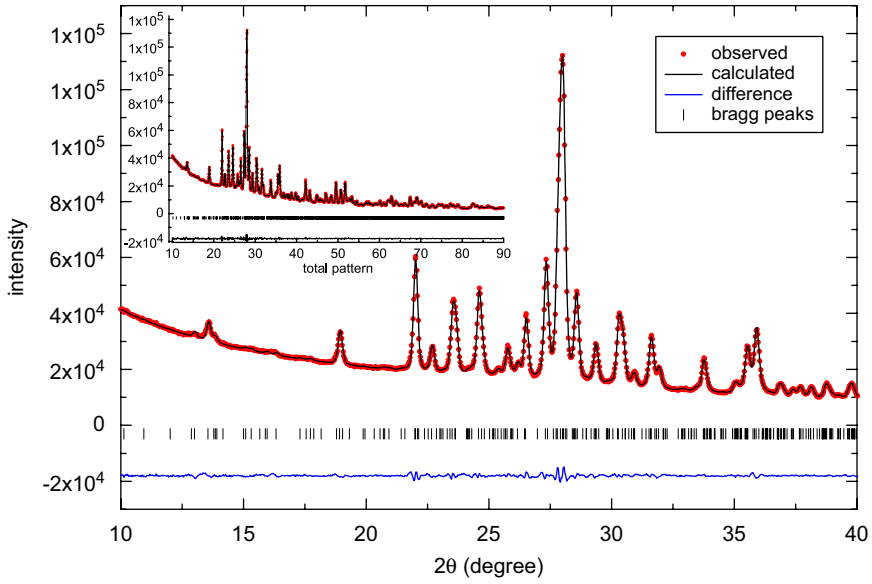

Fig. 2. Observed, calculated and difference X-ray diffraction pattern of an Eu-doped $CaAl_2Si_2O_8$ compound in the [10–40] 2θ range (in inset is given the total pattern).

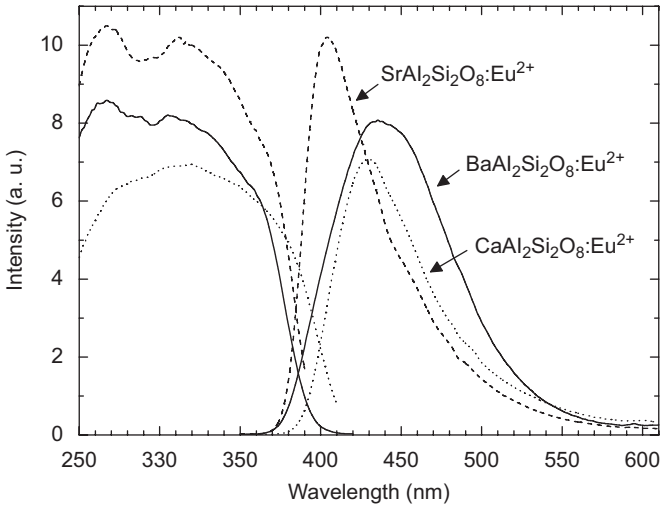

Fig. 3. Emission and excitation spectra of $M_{0.98}Eu_{0.02}Al_2Si_2O_8$ (M = Ca, Sr and Ba) collected at room temperature (λ_{exc} = 310 nm and λ_{em} = 430, 404 and 440 nm for Ca, Sr and Ba, respectively).

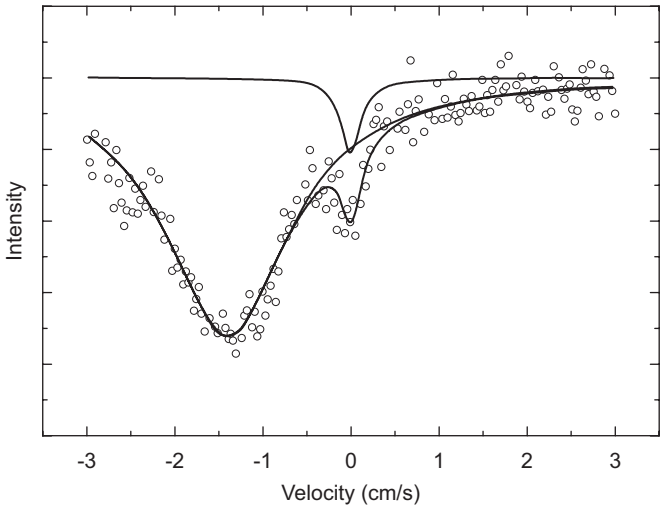

Fig. 4. ^{151}Eu Mössbauer absorption spectrum in $Ba_{0.95}Eu_{0.05}Al_2Si_2O_8$ recorded at 77 K.

Mössbauer spectroscopy (Fig. 4), synthesis conditions of $BaAl_2Si_2O_8$:Eu are not reductive enough to end at the complete reduction of Eu^{3+} into Eu^{2+}. Namely, the Mössbauer absorption spectrum of $Ba_{0.95}Eu_{0.05}Al_2Si_2O_8$ displays not only a broad line with an isomer shift (IS) of −14 mm/s assigned to Eu^{2+}, but also a clearly visible small intensity line with IS close to 0 mm/s assigned to Eu^{3+} [23]. Fitting these two components to Lorentzian-shaped lines reveals that there remains roughly 5–10% of Eu^{3+} in $Ba_{0.95}Eu_{0.05}Al_2Si_2O_8$, even after heating for 50 h in reducing atmosphere. Similar observations was recently reported for $SrAl_2O_4$:Eu 2%[24].

As aforementioned, the alkaline-earth cations sites in $MAl_2Si_2O_8$ (M = Ca, Sr and Ba) are 4, 1 and 1, respectively. Consequently, the emission peak of $BaAl_2Si_2O_8$:Eu^{2+} is naturally assigned to the unique crystallographic site available for Eu^{2+} cations and can be roughly simulated by a Gaussian curve when plotted in energy. A similar reasoning should also lead to a good fitting of the emission band in the case of $SrAl_2Si_2O_8$:Eu. Though, any attempts to match the 404 nm band by a Gaussian curve remained unsuccessful due to a strong asymmetry of the emission. This suggests that several Eu sites with slight differences in their chemical environments exist in $SrAl_2Si_2O_8$:Eu and should be accounted for the decomposition of the fluorescence spectrum. At first sight, this observation is quite surprising due to the ability of Eu^{2+} cations to accommodate Sr coordination for obvious steric reasons ($r(Sr^{2+})^{IX}$ = 1.31 Å and $r(Eu^{2+})^{IX}$ = 1.30 Å) [25], but could be explained on the basis of the existence of defects which may be coupled to some activators to give rise to phosphorescence (vide infra). In a similar way, based on the structural arrangement of the host lattice, the luminescent spectrum of $CaAl_2Si_2O_8$:Eu should exhibit four bands instead of the lonely one observed in Fig. 3. According to Park et al. [21], this broad emission might be deconvoluted in two contributions centered at 440 and 485 nm associated with the occupation of two different chemical sites by Eu^{2+} cations. The shift of the emission band to larger wavelength when Eu^{2+} concentration increases would be due to an enhancement in the energy transfer probability from one Eu site to another. The luminescence spectra of $Ca_{0.97}Eu_{0.03}Al_2Si_2O_8$, collected in fluorescence and phosphorescence modes, thanks to a CCD camera, are displayed in Fig. 5. Four emissions peaking at about

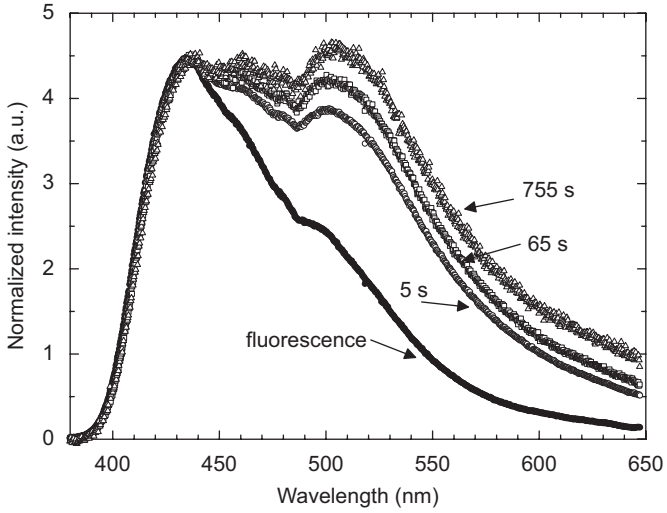

Fig. 5. Time evolution of the emission spectrum of $Ca_{0.97}Eu_{0.03}Al_2Si_2O_8$ after 5 s illumination at $\lambda_{exc} = 340$ nm. Spectra are normalized at $\lambda_{em} = 430$ nm.

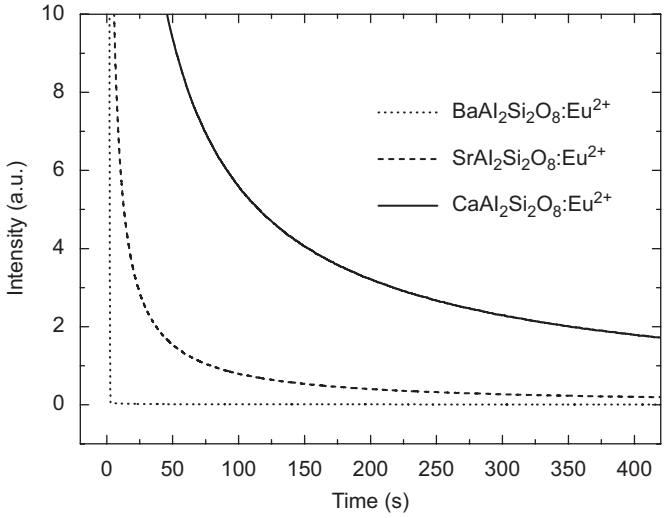

Fig. 6. Evolution of the emission in the phosphorescence mode of $Ca_{0.97}Eu^{2+}_{0.03}Al_2Si_2O_8$ ($\lambda_{em} = 430$ nm), $Sr_{0.97}Eu^{2+}_{0.03}Al_2Si_2O_8$ ($\lambda_{em} = 404$ nm) and $Ba_{0.97}Eu^{2+}_{0.03}Al_2Si_2O_8$ ($\lambda_{em} = 440$ nm) after 5 s illumination at $\lambda_{exc} = 350$ nm.

435, 460, 480 and 510 nm can clearly be identified on the fluorescence spectrum, which highlights the substitution of Ca for Eu at four distinct alkaline-earth sites. Nevertheless, as for the Sr phase, the difficulty to properly fit the emission spectrum with four Gaussian curves only suggests that extra Eu^{2+} sites should be considered. In fact, as discussed below and proposed by Clabau et al. [7], the much lower ionization potential (IP) of Eu^{2+} compared to Sr^{2+} and Ca^{2+} promotes the attractions of the electron acceptor oxygen vacancies by the activators (the polarization of the Eu^{2+} electron cloud towards the positively charged vacancy leads to some energy stabilization), which should induce in fluorescence the discrimination between activators with and without an associated defect. This trend is much less pronounced with Ba^{2+} due a lesser IP difference.

4. Phosphorescence of $MAl_2Si_2O_8:Eu^{2+}$ (M = Ca, Sr, Ba)

Persistent luminescence can be noticed for the three $MAl_2Si_2O_8$ hosts when doped with Eu^{2+}, a huge enhancement of the phosphorescence duration being observed when passing from Ba to Sr and Ca (Fig. 6). Namely, the $CaAl_2Si_2O_8:Eu^{2+}$ luminescence is perceivable with naked eyes up to 30 min after the excitation stop, and this phosphorescence duration may be extended up to 3 h with Pr^{3+} codoping [24]. The performances of the Eu-doped Ba and Sr derivatives and their codoped analogs are less impressive than those associated with the $CaAl_2Si_2O_8$ host lattice. Conditions favoring an increase of the phosphorescence duration in terms of synthesis route and chemical composition will be discussed somewhere else.

According to Clabau et al. [5,7,8] the afterglow mechanism in oxidizable lanthanide activator containing phosphors (i.e. Ce^{3+}, Eu^{2+}, Tb^{3+}, Pr^{3+}) excitable through a $4f \rightarrow 5d$ transition relies on a trapping of some electrons promoted to the activator $5d$ orbitals under UV excitation at a positively charged anionic vacancy $V_O^{\circ\circ}$ located in the vicinity of the luminescent centers. The return to the ground state is triggered by thermal energy supplied at room temperature via electron hopping to the photo-generated Eu^{3+} followed by a $4f^6 5d^1 \rightarrow 4f^7$ ($^8S_{7/2}$) radiative emission (Fig. 7). $V_O^{\circ\circ}$ defects positioned far away from photo-generated Eu^{3+} cations would not play the role of electron trap and would be inefficient in the phosphorescence mechanism. This model agrees with the evolution of the emission spectrum of $CaAl_2Si_2O_8:Eu^{2+}$ during phosphorescence. Indeed, once the excitation is stopped, the

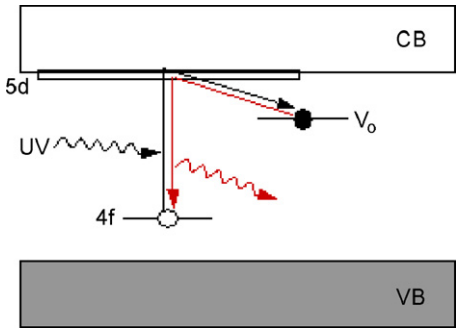

Fig. 7. Persistent luminescence mechanism proposed for phosphors associated with a $4f \rightarrow 5d$ excitation.

relative intensities of the four main luminescence peaks vary a lot, and a severe exaltation of the long wavelength emissions is observed with phosphorescence time (t) (Fig. 5). This goes along with modifications of the CIE x,y coordinates which shift from (0.17, 0.18) (for $t = 0$), to (0.22, 0.27), (0.22, 0.29) and (0.24, 0.30) for $Ca_{0.97}Eu_{0.03}Al_2Si_2O_8$ for $t = 5$, 65 and 755 s ($\lambda_{exc} = 340$ nm) [26], respectively. This change in the emission spectrum, going from fluorescence to phosphorescence, cannot originate from an energy transfer process. In fact, if electron traps were uncoupled to the activators, the de-trapped electrons should randomly migrate towards any activators via the conduction band. Accordingly, the time evolution of the luminescence intensity of the four, distinct Eu^{2+} cations should follow identical trends. As this is not the case, this implies that to some activator is associated a specific trap located in its neighborhood with a given depth as speculated by Clabau et al. [5,7] Consequently, to account for phosphorescence and fluorescence spectra (vide supra), Eu^{2+} cations coupled to an oxygen vacancy must be considered in addition to Eu^{2+} cations sitting at "unperturbed" alkaline-earth sites. Let us notice that this remark should be valid for others Eu^{2+} containing long persistent phosphors. However, according to the ability of the host lattice to deform, the europium surrounding, the nature of the traps, the phosphorescence mechanism, the phosphorescence duration, etc., the discrimination between emissions of activators at perturbed and unperturbed alkaline-earth sites may be difficult.

From an (probably) oversimplified model based on the use of the IPs of Eu^{2+} (i.e. 25 eV) and alkaline earth (i.e. 51.0, 43.7 and 37.4 eV for Ca, Sr and Ba, respectively) cations [27], the strength of the activator-oxygen vacancy interaction may be predicted. Namely, the positively charged anionic vacancies are supposed to be strongly attracted by activators with IP lower than the one of the alkaline earth they substitute for due to the ability of these activators to redistribute their electronic cloud to partially retrocede some negative charges to the vacancies and artificially to reduce the oxygen vacancy. Of course, such a stabilization goes along with change in the local environment of the rare earth and its crystal field which may induce modification in emission wavelength compared to an unperturbed chemical environment. The higher the IP difference ($\Delta IP(M^{2+}–Eu^{2+})$) between the alkaline-earth and Eu^{2+} cations, the stronger the attraction of the oxygen vacancy towards the lanthanide, the higher the stabilization of the conglomerated defects. As $\Delta IP(M–Eu)$ increases from Ba, to Sr and Ca, the oxygen vacancy—europium coupling is more efficient in Ca than in Sr and Ba containing materials, which favors the phosphorescence intensity and duration in Ca derivatives rather than in the Sr and Ba ones, as experimentally observed. Alternatively, the ability for oxygen defect to migrate nearby the activator makes controversial the deconvolution of the emission spectra into a given number of Gaussian curves equal to the strict number of crystal sites susceptible to accommodate lanthanide cations in the "undistorted" host lattice.

The mechanism of phosphorescence proposed by Clabau et al. [5,7,8] for the most outstanding phosphorescent material, $SrAl_2O_4:Eu^{2+},Dy^{3+}$ may be easily extended to $MAl_2Si_2O_8:Eu^{2+}$ compounds. The only difference lies in the value of the optical gap, much lower in the aluminosilicates than in the aluminate, which implies some readjustments in the relative positioning of the different energy levels involved in phosphorescence. In fact, diffuse reflectance measurements on $CaAl_2Si_2O_8$, $SrAl_2Si_2O_8$ and $BaAl_2Si_2O_8$ lead to optical gap of about 4 eV (i.e. ~4.1, 4.0 and 3.9 eV for Ba, Sr and Ca) against 6.5 eV for $SrAl_2O_4$ [28]. Moreover, XPS measurements carried out on $CaAl_2Si_2O_8$ and $Ca_{0.9}Eu_{0.1}Al_2Si_2O_8$ evidence that the highest occupied 4*f* levels of Eu^{2+} are located around 1 eV above the top of the valence band (Fig. 8). Consequently, the electronic structure of $CaAl_2Si_2O_8:Eu$, as its Sr and Ba congeners, may be schematized with Eu-*d* orbitals lying just below the conduction band and donor levels with a trap depth of approximately 0.4–0.6 eV for Ca, probably less for Sr and Ba due to their lower phosphorescence performance. This scheme would be coherent with the positioning of the Eu-5*d* levels by Dorenbos in numerous aluminates and derivatives. [6,29–31].

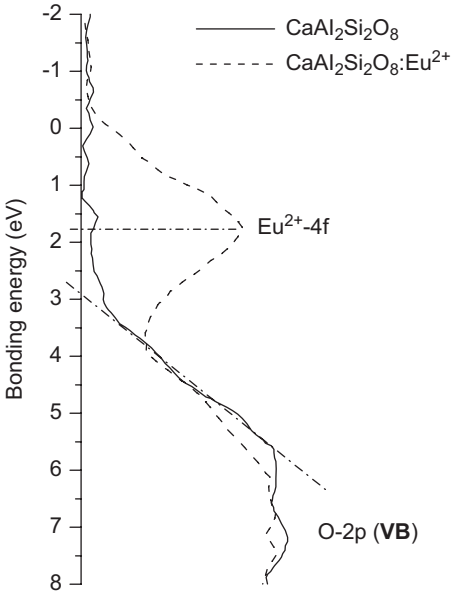

Fig. 8. XPS spectrum of $CaAl_2Si_2O_8$ and $Ca_{0.9}Eu_{0.1}Al_2Si_2O_8$.

5. Concluding remarks

The Eu^{2+}-doped $MAl_2Si_2O_8$ ($M = Ca$, Sr and Ba) aluminosilicates exhibit a bluish white luminescence which can last several minutes after the removal of the excitation, the phosphorescence duration increasing in the series $Ba < Sr \ll Ca$. The Eu^{2+} activators substitute for alkaline-earth cations and this substitution goes along with possible distortion of the local environment due to the ability of oxygen vacancies to migrate towards the Eu^{2+} lanthanide. This trend is more pronounced in $CaAl_2Si_2O_8$, compared to $SrAl_2Si_2O_8$ and $BaAl_2Si_2O_8$ due to a larger difference in $\Delta IP(M^{2+}–Eu^{2+})$ for Ca compared to Sr and Ba. The phosphorescence mechanism is associated with an electron trapping at oxygen vacancies located in the vicinity of the photo-ionized luminescent centers. The afterglow properties raises in the order $Ba < Sr \ll Ca$ due to the increasing difference in IP between Eu^{2+} and the alkaline-earth ions, and then to the attractiveness of the activators for anion vacancies and deeper traps. The evolution of the emission spectrum with phosphorescence duration is due to the coupling of luminescent centers with given traps with different depths.

Acknowledgment

The work at IMN was supported by Rhodia Electronics & Catalysis under Grant 9504213.00.

References

[1] Y. Murayama, Y. Aoki, N. Takeuchi, T. Matsuzawa, US Patent No. 5,424,006 (1995).
[2] T. Matsuzawa, Y. Aoki, N. Takeuchi, Y. Maruyama, J. Electrochem. Soc. 143 (1996) 2670.
[3] T. Aitasalo, P. Deren, J. Hölsa, H. Jungner, J. Krupa, M. Lastusaari, J. Legendziewicz, J. Niittykoski, W. Strek, J. Solid State Chem. 171 (2003) 114.
[4] C. Beauger, Thesis, Université de Nice, 1999.
[5] F. Clabau, X. Rocquefelte, S. Jobic, P. Deniard, M.-H. Whangbo, A. Garcia, T. Le Mercier, Chem. Mater. 17 (2005) 3904.
[6] P. Dorenbos, J. Electrochem. Soc. 152 (2005) H107.
[7] F. Clabau, X. Rocquefelte, T. Le Mercier, P. Deniard, S. Jobic, M. Whangbo, Chem. Mater. 18 (2006) 3212.
[8] F. Clabau, X. Rocquefelte, S. Jobic, P. Deniard, M.-H. Whangbo, A. Garcia, T. Le Mercier, Solid State Sci. 9 (2007) 608.
[9] T. Aitasalo, J. Hölsa, H. Jungner, M. Lastusaari, J. Niittykoski, J. Phys. Chem. B 110 (2006) 4589.
[10] M. Ohta, M. Maruyama, T. Hayakawa, T. Nishijo, J. Ceram. Soc. Japan 108 (2000) 284.
[11] Persistent luminescence is associated with the occurrence of a photo-generated metastable state under UV illumination. Namely, the phosphorescent decay time τ follows an exponential law, $1/\tau = s \exp(-E_T/kT)$, where s is a prefactor proportional to the vibration frequency of the trapped charge carrier within the trap (often taken to be equal to $10^{12}\,s^{-1}$), E_T the trap depth and k the Boltzman constant. If E_T equal 0.6 eV, then τ is 12 ms at room temperature, but ~1.2 s at 250 K, ~22 min at 200 K, ~4.5 years at 150 K and $\sim 55.10^9$ years at 100 K. Consequently, the notion of metastable state is quite relative since this state has to be stable enough on the chemical and thermodynamic points of view to last very long periods as soon as the temperature is lowered.
[12] Y. Lin, Z. Tang, Z. Zhang, Mater. Lett. 51 (2001) 14.
[13] B. Lei, Y. Liu, Z. Ye, C. Shi, J. Lumin. 109 (2004) 215.
[14] X. Wang, D. Jia, W. Yen, J. Lumin. 102 (2003) 34.
[15] X. Wang, Z. Zhang, Z. Tang, Y. Lin, Mater. Chem. Phys. 80 (2003) 1.
[16] R. McCauley, J. Mater. Sci. 35 (2000) 3939.
[17] S. Hong, J. Young, P. Yu, R. Kirkpatrick, J. Mater. Res. 14 (1999) 1828.
[18] X. Rocquefelte, F. Clabau, M. Paris, P. Deniard, T. Le Mercier, S. Jobic, M.H. Whangbo, Inorg. Chem. 46 (2007) 5456.
[19] T. Isaacs, J. Electrochem. Soc. 118 (1971) 1009.
[20] Y. Wang, Z. Wang, P. Zhang, F. Zhang, X. Fan, G. Qian, J. Rare Earths 23 (2005) 625.

[21] J.K. Park, J.M. Kim, E.S. Oh, C.H. Kim, Electrochem. Solid State Lett. 8 (2005) H6.
[22] W.-J. Yang, L. Luo, T.-M. Chen, N.-S. Wang, Chem. Mater. 17 (2005) 3883.
[23] G.K. Shenoy, F.E. Wagner, (Ed.), Mössbauer Isomer Shifts, North Holland, 1978.
[24] F. Clabau, Thesis, University of Nantes, France, 2005 (restricted distribution until 2010).
[25] R.D. Shannon, Acta Crystallogr. A 32 (1976) 751.
[26] The fluorescence spectrum of $Ca_{0.98}Eu_{0.02}Al_2Si_2O_8$ (Fig. 3) and $Ca_{0.97}Eu_{0.03}Al_2Si_2O_8$ (Fig. 5) are slightly different. This originates mainly from a change in chemical composition, the higher the Eu concentration, the higher the energy transfer probability. Moreover, let mention that an excitation wavelength of 340 nm instead of 310 nm will also favor an enhancement of the emission intensity of peaks at low energy. At the end, this difference might also stem from a change in the detector used to collect data (see experimental section).
[27] J. Emsley, The elements, Clarendon Press, Oxford, 1989.
[28] F. Pallila, A. Levine, M. Tomkus, J. Electrochem. Soc. 115 (1968) 642.
[29] P. Dorenbos, J. Phys.: Condens. Matter 17 (2005) 8103.
[30] P. Dorenbos, Chem. Mater. 17 (2005) 6452.
[31] A.V. Sidorenko, P. Dorenbos, A.J.J. Bos, C.W.E. van Eijk, P.A. Rodnyi, J. Phys.: Condens. Matter 18 (2006) 4503.